Supporting information

for

Hydrogen bonding interactions and supramolecular networks of pyridine-aryl based thiosemicarbazides and their Zn(II) complexes

Komala Pandurangan, Jonathan A. Kitchen, Thomas McCabe and Thorfinnur Gunnlaugsson*.

School of Chemistry, Trinity College Dublin and Trinity Biomedical Science Institute (TBSI), University of Dublin, Dublin 2, Ireland.

Thermal stability of [Zn(1)$_2$]·DMF 6

Thermal gravimetric analysis (TGA) was performed on red coloured crystalline [Zn(**1**)$_2$]·DMF **6**. Thermogram showed a gradual weight loss ~10% (20- 220ºC)[1-4] which corresponds to the loss of N,N-dimethyl formamide (DMF) from the pores of the crystalline **6**. The sharp weight loss from 220-350ºC most likely corresponds to the decomposition or partial sublimation of the Zn(II) complex. Further third sharp weight loss was observed in a range of 450-720ºC and is probably due to the complete decomposition of the complex **6** yielding Zinc oxide as a white solid. Both the sharp peaks attributes to the rest of the weight loss of the zinc complex **6**.

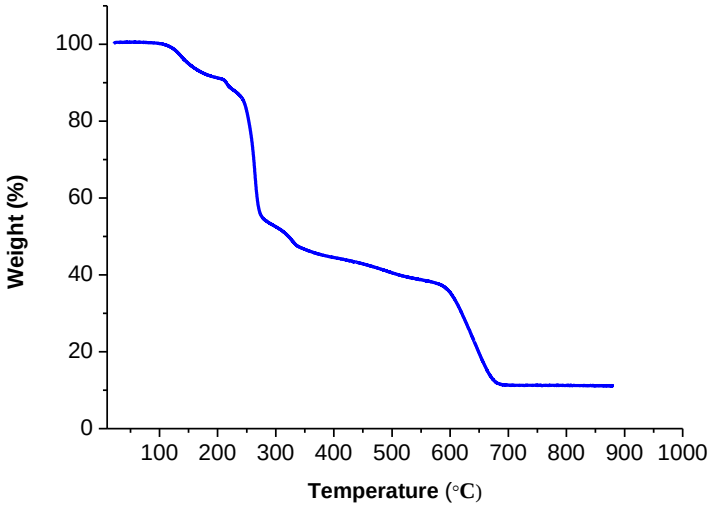

Fig S1: Thermal stability and thermogravimetric analysis (TGA) data for [Zn(**1**)$_2$]·DMF, **6** recorded in a nitrogen atmosphere.

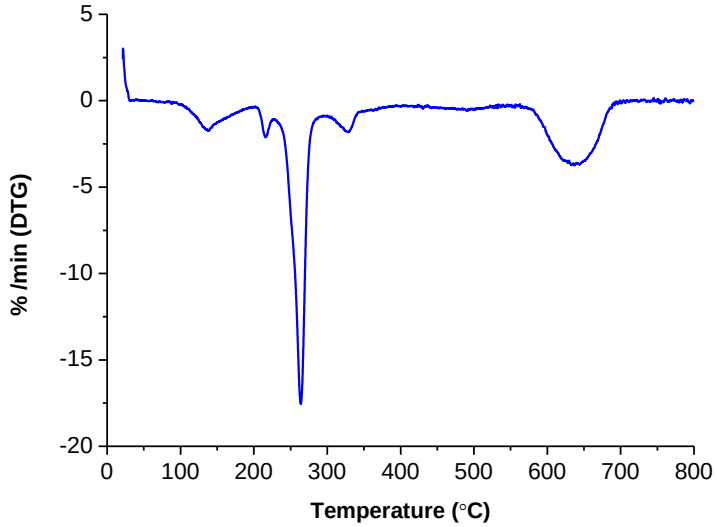

Fig S2: Thermal stability and derivative thermogravimetric analysis (DTGA) data for [Zn(**1**)$_2$]·DMF, **6**.

UV-Vis spectroscopic studies of Zn(II) complex 6 .

The spectroscopic studies of receptors **6** was carried out in acetonitrile using 1×10^{-5} M solution in the cell.

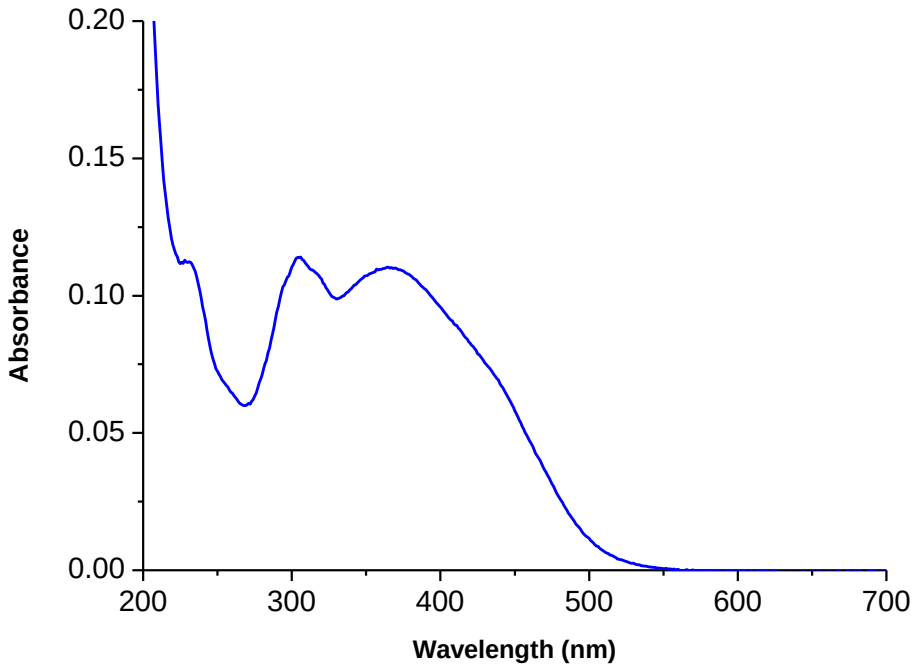

Fig S3: Absorption spectra of Zn(II)complex [Zn(**1**)$_2$]·DMF **6** in CH_3CN.

Packing diagram of 1-4

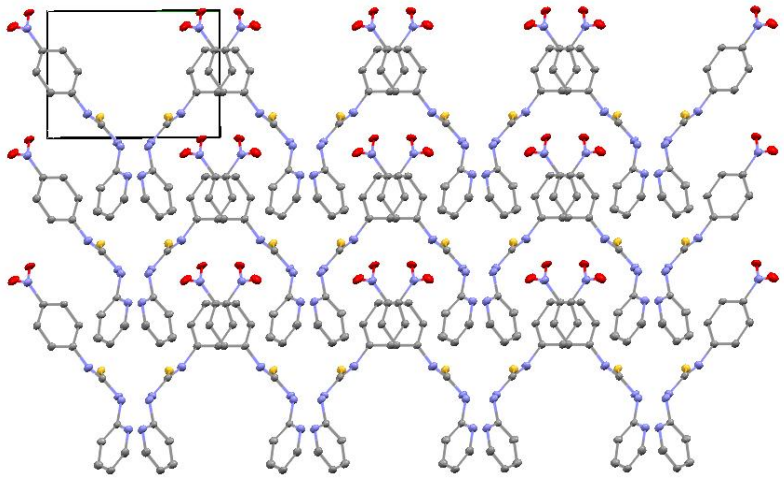

Fig S4: Packing diagram of thiourea **1** (view along c axis).

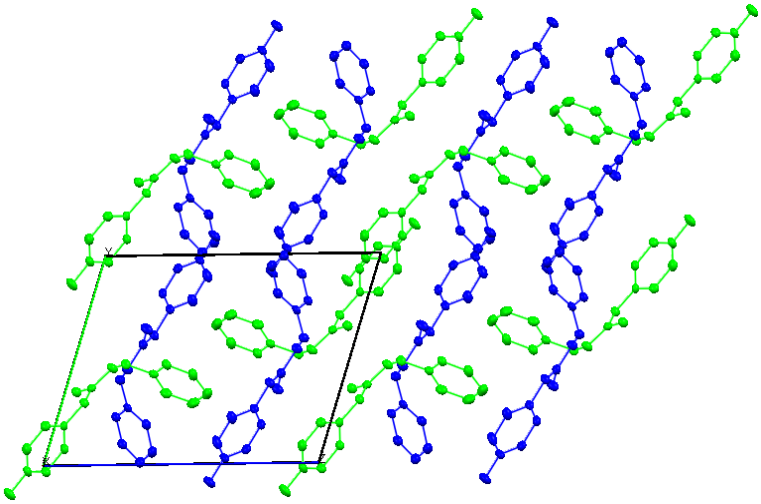

Fig S5: Packing diagram of **2** (view along axis a).

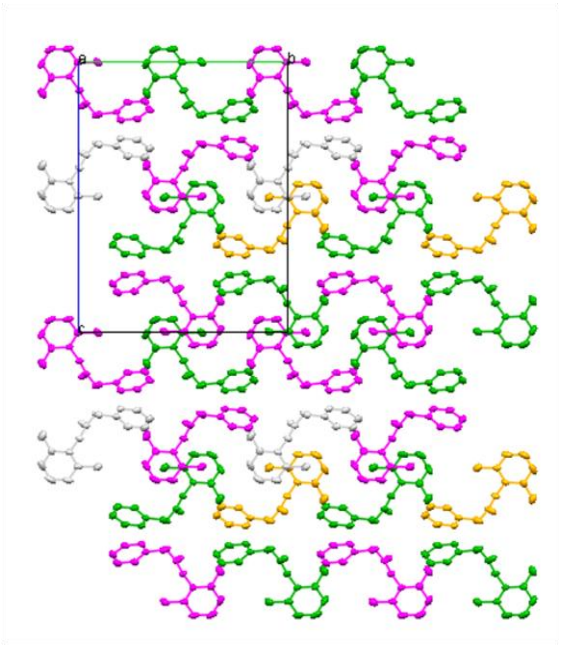

Fig S6: Packing diagram of **3**. (view along axis a)

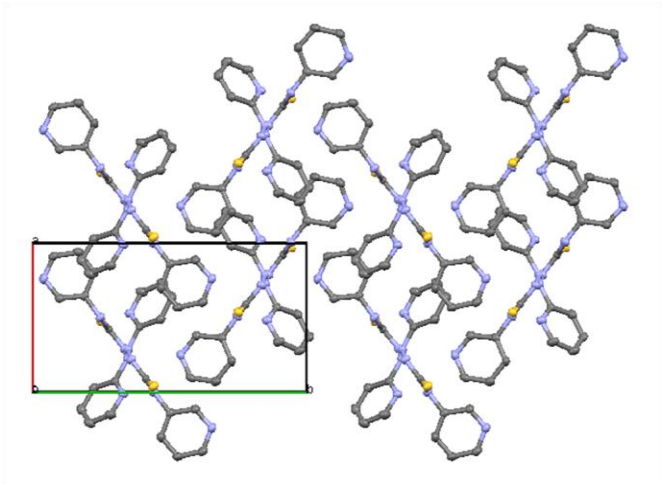

Fig S7: Packing diagram of thiourea **4** (view along c axis).

Table S1: Selected bond lengths [Å] **and bond angles**[°] **of 6 and 7**

Bond length		Bond angle	
Zinc complex 6			
Zn(1)-N(2)	1.9969(14)	N(2)-Zn(1)-S(1)	86.73(4)
Zn(1)-S(1)	2.2991(4)	N(2)#1-Zn(1)-S(1)	121.79(4)
		S(1)#1-Zn(1)-S(1)	124.18(2)
Zinc complex 7			
Zn(1)-N(2)	1.9969(14)	N(2)-Zn(1)-S(1)	86.73(4)
Zn(1)-S(1)	2.2991(4)	N(2)#1-Zn(1)-S(1)	121.79(4)
		S(1)#1-Zn(1)-S(1)	124.18(2)

Void analysis of 6 and 7

Table S2: Calculated values of cavity volumes for contact surface of $[Zn(1)_2]$ [a] and $[Zn(5)_2]$

	$[Zn(\mathbf{1})_2]$, **6** [a]	$[Zn(\mathbf{5})_2]$, **7**
Probe radius **(**Å)	Void volume (Å^3)	Void volume (Å^3)
1.7	432.75 (13.8)	261.11 (8.2)
1.6	453.40 (14.5)	323.78 (10.1)
1.5	491.99 (15.7)	354.73 (11.1)
1.4	521.98 (16.7)	383.55 (12.0)
1.3	542.42 (17.3)	462.45 (14.5)
1.2	615.10 (19.7)	487.42 (15.3)

[a] Squeeze command was used to remove the disordered DMF.

References:

1) Roberts, J. M.; Fini, B. M.; Sarjeant, A. A.; Farha, O. K.; Hupp, J. T.; Scheidt, K. A. *J. Am. Chem. Soc.*, **2012**, *134*, 3334.
2) Chen, B.; Wang, X.; Zhang, Q.; Xi, X.; Cai, J.; Qi, H.; Shi, S.; Wang, J.; Yuan, D.; Fang, M. *J. Mater. Chem.*, **2010**, *20*, 3758.
3) Sapchenko, S. A.; Dybtsev, D. N.; Samsonenko, D. G.; Fedin, V. P. *New J. Chem.*, **2010**, *34*, 2445.
4) Pachfule, P.; Das, R.; Poddar, P.; Banerjee, R. *Crystal Growth & Design* **2011**, *11*, 1215.